Northumbria Research Link

www.northumbria.ac.uk/nrl

northumbria
UNIVERSITY NEWCASTLE

Vibration and Lateral Buckling Optimisation of Thin-walled Laminated Composite Channel-section Beams

Hoang X. Nguyen[a], Jaehong Lee[b,*], Thuc P. Vo[a,*], Domagoj Lanc[c]

[a]*Department of Mechanical and Construction Engineering, Northumbria University, Newcastle upon Tyne NE1 8ST, United Kingdom*
[b]*Department of Architectural Engineering, Sejong University, 98 Gunja Dong, Gwangjin Gu, Seoul 143-747, South Korea*
[c]*Department of Engineering Mechanics, Faculty of Engineering, University of Rijeka, Vukovarska 58, HR-51000 Rijeka, Croatia.*

Abstract

This study presents vibration and lateral buckling optimisation of thin-walled laminated composite beams with channel sections. While flanges' width, web's height, and fibre orientation are simultaneously treated as design variables, the objective function involves maximising the fundamental frequency and critical buckling moment. Based on the classical beam theory, the beam element with seven degrees of freedom at each node is developed to solve the problem. Micro Genetic Algorithm (micro-GA) is then employed as an optimisation tool to obtain optimal results. A number of composite channel-section beams with different types of boundary conditions, span-to-height ratios, and lay-up schemes are investigated for the optimum design. The outcomes reveal that geometric parameters severely govern the optimal solution rather than the fibre orientation and it is considerably effective to use micro-GA compared with regular GA in term of optimal solution and convergence rate.

Keywords: Thin-walled composite beams; Micro Genetic Algorithm; Finite element

*Corresponding author
   Email addresses:* `hoangnguyence@gmail.com` (Hoang X. Nguyen), `jhlee@sejong.ac.kr` (Jaehong Lee), `thuc.vo@northumbria.ac.uk` (Thuc P. Vo), `dlanc@riteh.hr` (Domagoj Lanc)

1. Introduction

Composite material has been intensively used over the last decades in variety of fields of architectural, civil, mechanical, aeronautical engineering which require high strength and stiffness with relatively low material weight. Composite material also possesses high tailorability enabling engineers to adjust their designs optimising laminate configuration, in association with geometric shapes, to meet specific requirements. Being an essential element in many engineering structures, thin-walled laminated composite beams with open cross-section are widely used. These beams might be subjected to different types of external forces and boundary conditions causing vibration and buckling in various modes which they are absolutely susceptible. This requires reliable analysis approach to predict their vibration and stability responses.

Since the early work of Bauld and Tzeng [1], many studies have been done to develop appropriate models for vibration [2–12] and lateral buckling problems [13–20] of thin-walled composite beams and only a few of them are cited here. More details of these works can be found in some books written by Kollar and Springer [21], Librescu and Song [22], and Hodges [23]. With regard to optimisation problems, Szymcazak [24] proposed a procedure of optimum weight design of thin-walled I-section beam for a provided frequency. Magnucki [25] optimised cold-form thin-walled beams with open cross-section for strength, stability, and geometric conditions. For thin-walled composite beams, Morton and Webber [26] developed analytic procedure to obtain an optimal solution of I-section beams with failure, local buckling and deflection constraints. Davalos and Qiao [27] presented multiobjective design optimisation formulation to optimise composite I-section beams with respect to fibre orientations and fibre percentages. Walker [28] studied optimal design of composite I-section beams for a maximum combination of crippling, buckling load and postbuckling strength. Savic et al. [29] optimised maximum bending and axial stiffness of composite I-section beams by using fibre angles as design variables. Rajasekaran [30] applied evolution strategies to find minimum weight design of thin-walled composite beams.

Genetic Algorithm (GA) is widely considered as an effective optimisation tool in term

of solution reliability and convergence rate. This algorithm which has become popular after the work of Holland [31] is inspired by the process of natural election. This non-gradient stochastic optimisation algorithm is suitable for those problems whose design variables are discrete values rather than continuous ones. Micro-GA enhances the performance of regular GA in convergence rate by performing elitism to generate a new population of each iteration. This improvement effectively increases the optimal solution and convergence rate of the optimising procedure which results in significant reduction in computational cost. Recently, Nguyen et al. [32] presented an optimisation study of composite I-section beams by maximising the critical flexural-torsional buckling load using micro-GA. As far as authors are aware, there is no work available on the optimum design of composite channel-section beams using mirco-GA for vibration and lateral buckling problems.

In this study, in order to fill the aforementioned gap, vibration and lateral buckling optimisations of thin-walled composite beams with channel-section, in which both cross-section shape and laminate configuration are varied at the same time, are investigated. The beam element with seven degrees of freedom at each node is developed to analyse composite beams and then micro-GA is employed as a searching engine to obtain optimisation results. Numerical examples are presented to investigate optimum design of composite channel-section beams with various configurations such as boundary conditions, span-to-height ratios, and lay-up schemes. The effectiveness of the micro-GA compared with regular GA in term of optimal solution and convergence rate is discussed.

2. Theoretical formulation

In this section, theoretical formulation for vibration and lateral buckling analysis of thin-walled composite beams is briefly summarised and more details of this part can be found in Refs.[7, 16]. The different coordinates system are presented in the Fig. 1.

2.1. Displacement field

Based on the classical lamination theory, the out of mid-line displacement components u, v, w are as follow:

$$u\left(s, z, n\right) = \overline{u}\left(s, z\right) \tag{1a}$$

$$v\left(s, z, n\right) = \overline{v}\left(s, z\right) - n\frac{\partial \overline{u}\left(s, z\right)}{\partial s} \tag{1b}$$

$$w\left(s, z, n\right) = \overline{w}\left(s, z\right) - n\frac{\partial \overline{u}\left(s, z\right)}{\partial s} \tag{1c}$$

where the mid-surface displacements $\overline{u}, \overline{v}, \overline{w}$ in the contour coordinate with respect to the displacements U, V of the pole P in Cartesian coordinate system and the rotation angle Φ about the pole axis are given as:

$$\overline{u}\left(s, z\right) = U\left(z\right)\sin\theta\left(s\right) - V\left(z\right)\cos\theta\left(s\right) - \Phi\left(z\right)q\left(s\right) \tag{2a}$$

$$\overline{v}\left(s, z\right) = U\left(z\right)\cos\theta\left(s\right) + V\left(z\right)\sin\theta\left(s\right) + \Phi\left(z\right)r\left(s\right) \tag{2b}$$

$$\overline{w}\left(s, z\right) = W(z) - U'(z)x(s) - V'(z)y(s) - \Phi'(z)\omega(s) \tag{2c}$$

where prime $(')$ denotes the differentiation with respect to z, W is axial displacement and ω represents warping function:

$$\omega\left(s\right) = \int r\left(s\right) ds \tag{3}$$

The non-zero strains are given by:

$$\epsilon_z = W' - \left(x + n\sin\theta\right)U'' - \left(y - n\cos\theta\right)V'' - \left(\omega - nq\right)\Phi'' \tag{4a}$$

$$\gamma_{sz} = 2n\Phi' \tag{4b}$$

2.2. Governing equations

The constitutive equation for thin-walled composite beams is of the form:

$$\begin{Bmatrix} N_z \\ M_y \\ M_x \\ M_\omega \\ M_t \end{Bmatrix} = \begin{bmatrix} E_{11} & E_{12} & E_{13} & E_{14} & E_{15} \\ & E_{22} & E_{23} & E_{24} & E_{25} \\ & & E_{33} & E_{34} & E_{35} \\ & & & E_{44} & E_{45} \\ sym. & & & & E_{55} \end{bmatrix} \begin{Bmatrix} W' \\ -U'' \\ -V'' \\ -\Phi'' \\ 2\Phi' \end{Bmatrix} \tag{5}$$

4

where E_{ij} are the stiffness components of thin-walled composite beams and $N_z, M_y, M_x, M_\omega, M_t$ are the stress resultants defined by:

$$N_z = \int_A \sigma_z \, ds \, dn \tag{6a}$$

$$M_y = \int_A \sigma_z \left(x + n \sin \theta \right) ds \, dn \tag{6b}$$

$$M_x = \int_A \sigma_z \left(y - n \cos \theta \right) ds \, dn \tag{6c}$$

$$M_\omega = \int_A \sigma_z \left(\omega - nq \right) ds \, dn \tag{6d}$$

$$M_t = \int_A \sigma_{sz} n \, ds \, dn \tag{6e}$$

The governing equations of thin-walled composite beams for free vibration and lateral buckling problems are obtained as:

$$N_z' = m_0 \ddot{W} \tag{7a}$$

$$M_y'' + (M_b \Phi)'' = m_0 \ddot{U} + (m_c + m_0 y_p) \ddot{\Phi} \tag{7b}$$

$$M_x'' = m_0 \ddot{V} + (m_s - m_0 x_p) \ddot{\Phi} \tag{7c}$$

$$M_\omega'' + 2M_t' + M_b U'' = (m_c + m_0 y_p) \ddot{U} + (m_s - m_0 x_p) \ddot{V} + (m_p + m_2 - 2m_\omega) \ddot{\Phi} \tag{7d}$$

where $m_0, m_c, m_s, m_p, m_2, m_\omega$ are inertia coefficients and M_b denotes buckling moment.

The explicit form of the governing equations can be expressed:

$$E_{11} W'' - E_{12} U''' - E_{13} V''' - E_{14} \Phi''' + 2E_{15} \Phi'' = m_0 \ddot{W} \tag{8a}$$

$$E_{12} W''' - E_{22} U^{IV} - E_{23} V^{IV} - E_{24} \Phi^{IV} + 2E_{25} \Phi''' + (M_b \Phi)'' = m_0 \ddot{U} + (m_c + m_0 y_p) \ddot{\Phi} \tag{8b}$$

$$E_{13} W''' - E_{23} U^{IV} - E_{33} V^{IV} - E_{34} \Phi^{IV} + 2E_{35} \Phi''' = m_0 \ddot{V} + (m_s - m_0 x_p) \ddot{\Phi} \tag{8c}$$

$$E_{14} W''' - E_{24} U^{IV} - E_{34} V^{IV} - E_{44} \Phi^{IV} + 2E_{15} W'' - 2E_{25} U''' - 2E_{35} V''' + 4E_{55} \Phi'' + M_b U''$$

$$= (m_c + m_0 y_p) \ddot{U} + (m_s - m_0 x_p) \ddot{V} + (m_p + m_2 - 2m_\omega) \ddot{\Phi} \tag{8d}$$

2.3. Finite element formulation

The beam element with seven degrees of freedom at each node is used. The displacements are expressed over each element as a combination of the linear Lagrange interpolation function Ψ_j and Hermite-cubic interpolation function ψ_j associated with node j and the nodal values:

$$W = \sum_{j=1}^{2} w_j \Psi_j \tag{9a}$$

$$U = \sum_{j=1}^{4} u_j \psi_j \tag{9b}$$

$$V = \sum_{j=1}^{4} v_j \psi_j \tag{9c}$$

$$\Phi = \sum_{j=1}^{4} \phi_j \psi_j \tag{9d}$$

The finite element model of a typical element can be expressed:

$$([K] - M_b[G] - \omega^2[M])\{\Delta\} = \{0\} \tag{10}$$

where $[K], [G]$ and $[M]$ are the element stiffness, geometric stiffness, mass matrix, respectively and $\{\Delta\}$ represents the eigenvector of nodal displacements corresponding to an eigenvalue:

$$\{\Delta\} = \{W\ U\ V\ \Phi\}^{\mathrm{T}} \tag{11}$$

3. Formulation of optimisation problem

Due to high tailorability of composite materials, engineers are able to adjust laminate configurations to accomplish highest structural responses which sufficiently meet specific design requirements. Moreover, channel sections enable engineers to optimise structures' performance even further by providing additional possibilities of varying geometric parameters, e.g. web's height and flanges' width as shown in Fig. 2. Following those aforementioned observations, the optimisation of composite channel-section beams for vibration and lateral buckling problems could be defined as follow:

6

Find:

$$\theta, d, b$$

Maximise:

$$\mathcal{H}(\theta, d, b)$$

Subjected to:

$$\frac{A}{A*} \leq 1 \tag{12a}$$

$$\frac{d}{b} \geq 1 \tag{12b}$$

$$10 \leq \frac{L}{d} \leq 100 \tag{12c}$$

where design variables of (θ, d, b) are fibre orientation, web's height, and flanges' width, respectively. $\mathcal{H}$ represents objective function of the fundamental frequencies or critical buckling moments of beams. A and A^* are cross-sectional area and its allowable upper value, respectively. L denotes the beam's length.

In order to be implemented in the optimisation procedure using micro-GA, non-constrained optimisation problem should be introduced by transforming from the above constrained one. As a result, optimisation problem could be equivalently redefined as follow:

Find:

$$\theta, d, b$$

Maximising:

$$\mathcal{G}(\theta, d, b) = \mathcal{H} - [\gamma_1(A/A^* - 1)^2 + \gamma_2(1 - d/b)^2 + \gamma_3(\beta - L/d)^2] \tag{13}$$

where γ_1, γ_2 and γ_3 represent penalty parameters which are assigned positive values if the corresponding constraints are violated. β denotes the upper bound or lower bound constraint of L/d (Eq. 12c) and $\mathcal{G}$ is newly defined objective function which includes the initial objective function $\mathcal{H}$ and the penalty term. It should be noted that each penalty parameter is set as zero if the corresponding constraint is satisfied.

7

4. Numerical examples and discussion

In this section, the verification is carried out to illustrate the validity and accuracy of the analysis procedure in Section 2. It is followed by the optimisation of composite channel-section beams for the vibration and lateral buckling under pure bending problems. Three types of boundary conditions including simply-supported (S-S), clamped-clamped (C-C), and clamped-free (C-F) with various beam's lengths are investigated. For all analysis and optimisation cases, eight beam elements are used.

4.1. Verification

For verification purpose, firstly, vibration analysis of S-S channel-section beams is tested and compared with the results reported by Cortinez and Piovan [4] and Prokic et al. [11]. Graphite-epoxy (AS4/350), whose material properties are $E_1 = 144$ GPa, $E_2 = E_3 = 9.65$ GPa, $G_{12} = G_{13} = 4.14$ GPa, $G_{23} = 3.45$ GPa, $\nu_{12} = \nu_{13} = 0.3$, $\nu_{23} = 0.5$, is used for this example. While the flanges' width and web's height of the channel-section beams are equally assigned as 0.6 m, its total thicknesses which consist of 4 plies are 0.03 m. As can be seen in the Table 1, the fundamental frequencies obtained from present study are in good agreement with those of previous published works. Secondly, several attempts are conducted to verify the lateral buckling analysis of cantilever channel-section beams under pure bending moments. The material properties of glass-epoxy are $E_1 = 53.78$ GPa, $E_2 = E_3 = 17.93$ GPa, $G_{12} = G_{13} = 8.96$ GPa, $G_{23} = 3.45$ GPa, $\nu_{12} = \nu_{13} = 0.25$, $\nu_{23} = 0.34$. A 4m-long beam whose flanges' width and web's height are 25 mm and 50 mm, respectively, is considered. A number of unidirectional, symmetric angle-ply and cross-ply laminates whose all thicknesses are 2.08 mm are investigated. As shown in the Table 2, the present results are considerably acceptable compared to those of Kim et al. [19]. Apparently, the verification of vibration and lateral buckling problems has confirmed the validity and reliability of the present study.

4.2. Vibration optimisation of composite channel-section beams

In this example, vibration optimisation of composite channel-section beams, whose geometry is shown in Fig. 2, is conducted. Material properties and prescribed geometric

parameters of the beams are given in the Table 3. The geometric design variables of flanges' width and web's height vary from 15 mm to 300 mm with the interval of 5 mm while those of fibre angles are allowed to change in the step of 1^0 from 0^0 to 90^0. Consequently, geometric and fibre variables possess 58 and 91 possibilities resulting in 6 and 7 genes of chromosome length to be used in GA optimisation, respectively. Other micro-GA parameters are given in Table 4. For each type of boundary condition (S-S, C-C and C-F), there are three different symmetric laminated configurations of $[\theta_1/-\theta_1]_{4s}$, $[\theta_1/-\theta_2]_{4s}$, and $[\theta_1/-\theta_1/\theta_2/-\theta_2]_{2s}$ are considered. In order to illustrate the effectiveness of the proposed optimisation procedure, vibration analysis results of assumed regular design, whose geometric properties are all satisfied the constraints in Eq. (12a), with unidirectional fibre angle and fixed flanges' width and web's height of 50 mm and 100 mm, respectively, are provided.

As can be observed in the Table 5, all optimal design cases with geometric and fibre angle variables yield considerably higher results compared to those of regular design in term of the objective function of fundamental frequency. Furthermore, due to its high flexibility in choosing values for the design variable of fibre angles, the generated solutions from $[\theta_1/-\theta_2]_{4s}$ and $[\theta_1/-\theta_1/\theta_2/-\theta_2]_{2s}$ laminate configurations are relatively better than those of $[\theta_1/-\theta_1]_{4s}$ lay-ups. The optimisation results in Table 5 are also visually demonstrated in Figs. 3-5. For each graph, the relation of the beam's length and optimal fundamental frequency is provided by adding the cross-section shape of optimal designs. The assumed regular designs are given for comparison purpose only. As seen for all cases, the growth of beam's length is followed by the decline of optimal fundamental frequency which confirms the fact that structures, in general, become weaker as their span get longer.

Similarly, the optimisation solutions for C-C and C-F beams, which are given in Tables 6 and 7, follow the same trend of S-S beams. All variable laminates yield optimal amount of fundamental frequency ranging from $(10\% - 29\%)$ and $(23\% - 24\%)$ higher than that of regular designs. Furthermore, among the selected lay-ups, due to its flexibility in choosing fibre angle, the $[\theta_1/-\theta_1/\theta_2/-\theta_2]_{2s}$ lay-up always exhibits the highest optimal results while the $[\theta_1/-\theta_1]_{4s}$ lay-up shows the lowest ones. In addition, the obtained optimal fibre angles are smaller than 45^0 for all cases enabling the possibility to reduce upper bound of fibre

angle range from 90^0 to 45^0 in practical problems. This would lead to a significant reduction in GA search space resulting in faster converged solutions obtained.

It should be noted that, in each case of boundary condition, the identical optimal values of flange's width b and web's height d are obtained for the same beam's length regardless of variable laminates. For instance, with S-S beams (Table 5), the solutions of $b = 60$ mm and $d = 80$ mm obtaining for $L = 4$ m and $L = 12$ m are maintained for all three different laminated configurations. This clearly reveals that the geometric parameters including flanges' width, web's height, and beam's length play crucial roles in optimal design of composite channel-section beams for vibration problem rather than fibre orientations.

4.3. Lateral buckling optimisation of composite channel-section beams

In this part, several examples of lateral buckling optimisation of composite channel-section beams under pure bending moments are presented. The material properties, geometric and GA parameters stay the same with those of previous part. Tables 8-10 present the lateral buckling optimisation results for the S-S, C-C, and C-F beams, respectively. Similar trends as vibration optimisation problem are observed. All optimal critical buckling moments of variable laminates are markedly higher than regular design for the same length of beam. Among those, the most effective lay-up with the highest values of critical buckling moment belongs to $[\theta_1/-\theta_1/\theta_2/-\theta_2]_{2s}$. Interestingly, for all types of different boundary conditions, the solutions for optimal geometric variables of b and d are mostly 65 mm and 70 mm, respectively, except the case for $L = 12$ m which would violate the third constraint (Eq. 12c) if $d = 70$ mm. This has reconfirmed that geometric parameters are critical factors which govern the optimisation results of not only vibration but also the lateral buckling problem. The illustrations of the data in Table 8 for the S-S beams are given in the Figs. 6-8.

Finally, in order to demonstrate the effectiveness of the micro-GA in finding optimal results, the convergence history of regular GA and micro-GA for vibration optimisation of a 6m-long S-S beam with $[\theta_1/-\theta_1]_{4s}$ lay-up is presented in Fig. 9. It is observed that for the same initial parameters which provided in Table 4, while the regular GA requires around

10

29 generations to converge, only 21 generations are needed for micro-GA. Besides, it is also interesting to note that the objective function of micro-GA is approximately 5% better than that of regular GA.

5. Conclusions

In this study, formulation and procedure for optimisation of thin-walled composite beams with channel section are presented. Objective functions for two type of problems are maximisation of fundamental frequency and critical buckling moment while flanges' width, web's height, and fibre angle are simultaneously considered as design variables. The optimisation results apparently show that optimal solutions are crucially governed by geometric parameters such as length of beam, flanges' width, and web's height rather than the laminate configuration including lay-up scheme and fibre orientation. In addition, the micro-GA has evidently proved its advantages over the regular GA in term of convergence rate and optimal objective value meaning that micro-GA is able to yield better optimisation result in faster convergence rate than that of regular GA.

References

[1] N. R. Bauld Jr., T. Lih-Shyng, A Vlasov theory for fiber-reinforced beams with thin-walled open cross sections, International Journal of Solids and Structures 20 (3) (1984) 277–297.

[2] X. X. Wu, C. T. Sun, Vibration analysis of laminated composite thin-walled beams using finite elements, AIAA Journal 29 (5) (1991) 736–742.

[3] D. H. Hodges, A. R. Atilgan, M. V. Fulton, L. W. Rehfield, Free-vibration analysis of composite beams, Journal of the American Helicopter Society 36 (3) (1991) 36–47.

[4] V. H. Cortinez, M. T. Piovan, Vibration and Buckling of Composite Thin-Walled Beams with Shear Deformability, Journal of Sound and Vibration 258 (4) (2002) 701–723.

[5] M. T. Piovan, V. H. Cortinezz, Mechanics of shear deformable thin-walled beams made of composite materials, Thin-Walled Structures 45 (1) (2007) 37 – 62.

[6] J. Lee, S.-E. Kim, Free vibration of thin-walled composite beams with I-shaped cross-sections, Composite Structures 55 (2) (2002) 205–215.

[7] J. Lee, S.-E. Kim, Flexural-torsional coupled vibration of thin-walled composite beams with channel sections, Computers & Structures 80 (2) (2002) 133–144.

[8] T. P. Vo, J. Lee, Flexural-torsional coupled vibration and buckling of thin-walled open section composite beams using shear-deformable beam theory, International Journal of Mechanical Sciences 51 (9-10) (2009) 631–641.

[9] T. P. Vo, J. Lee, On triply coupled vibrations of axially loaded thin-walled composite beams, Computers and Structures 88 (3-4) (2010) 144–153.

[10] T. P. Vo, J. Lee, K. Lee, N. Ahn, Vibration analysis of thin-walled composite beams with I-shaped cross-sections, Composite Structures 93 (2) (2011) 812–820.

[11] A. Prokic, D. Lukic, I. Milicic, Free Vibration Analysis of Cross-Ply Laminated Thin-Walled Beams with Open Cross Sections: Exact Solution, Journal of Structural Engineering 139 (4) (2013) 623–629.

[12] P. R. Heyliger, Elasticity-based free vibration of anisotropic thin-walled beams, Thin-Walled Structures 95 (2015) 73 – 87.

[13] J. T. Mottram, Lateral-torsional buckling of thin-walled composite I-beams by the finite difference method, Composites Engineering 2 (2) (1992) 91 – 104.

[14] A. N. Sherbourne, M. Kabir, Shear Strain Effects in Lateral Stability of Thin-Walled Fibrous Composite Beams, Journal of Engineering Mechanics 121 (5) (1995) 640–647.

[15] D. H. Hodges, D. A. Peters, Lateral-torsional buckling of cantilevered elastically coupled composite strip- and I-beams, International Journal of Solids and Structures 38 (9) (2001) 1585–1603.

[16] J. Lee, S.-E. Kim, Lateral buckling analysis of thin-walled laminated channel-section beams, Composite Structures 56 (4) (2002) 391–399.

[17] S. P. Machado, V. H. Cortinez, Lateral buckling of thin-walled composite bisymmetric beams with prebuckling and shear deformation, Engineering Structures 27 (8) (2005) 1185 – 1196.

[18] V. H. Cortinez, M. T. Piovan, Stability of composite thin-walled beams with shear deformability,

Computers and Structures 84 (15-16) (2006) 978 – 990.

[19] N.-I. Kim, D. K. Shin, M.-Y. Kim, Exact lateral buckling analysis for thin-walled composite beam under end moment, Engineering Structures 29 (8) (2007) 1739–1751.

[20] D. Lanc, G. Turkalj, I. Pesic, Global buckling analysis model for thin-walled composite laminated beam type structures, Composite Structures 111 (0) (2014) 371 – 380.

[21] L. P. Kollar, G. S. Springer, Mechanics of Composite Structures, Cambridge University Press, 2003.

[22] L. Librescu, O. Song, Thin-Walled Composite Beams: Theory and Application (Solid Mechanics and Its Applications), Kluwer Academic Pub, 2006.

[23] D. H. Hodges, Nonlinear composite beam theory, Progress in astronautics and aeronautics 213 (2006) 304.

[24] C. Szymczak, Optimal design of thin-walled I beams for a given natural frequency of torsional vibrations, Journal of Sound and Vibration 97 (1) (1984) 137–144.

[25] K. Magnucki, Optimization of open cross section of the thin-walled beam with flat web and circular flange, Thin-Walled Structures 40 (3) (2002) 297–310.

[26] S. K. Morton, J. P. H. Webber, Optimal design of a composite I-beam, Composite Structures 28 (2) (1994) 149–168.

[27] J. F. Davalos, P. Qiao, E. J. Barbero, Multiobjective material architecture optimization of pultruded FRP I-beams, Composite Structures 35 (3) (1996) 271–281.

[28] M. Walker, Multiobjective optimisation of laminated I-beams for maximum crippling, buckling and postbuckling strength, Composites Part B: Engineering 29 (3) (1998) 263–270.

[29] V. Savic, M. E. Tuttle, Z. B. Zabinsky, Optimization of composite I-sections using fiber angles as design variables, Composite Structures 53 (3) (2001) 265–277.

[30] S. Rajasekaran, Optimal laminate sequence of non-prismatic thin-walled composite spatial members of generic section, Composite Structures 70 (2) (2005) 200 – 211.

[31] J. H. Holland, Adaptation in natural and artificial systems: an introductory analysis with applications to biology, control, and artificial intelligence, MIT press, 1975.

[32] X.-H. Nguyen, N.-I. Kim, J. Lee, Optimum design of thin-walled composite beams for flexural-torsional buckling problem, Composite Structures 132 (2015) 1065–1074.

Tables

Table 1: Fundamental frequencies of simply-supported composite channel-section beams (Hz)

Lay-ups	h/L	L (m)	This study	Ref. [4]	Ref. [11]
$[0^0]_4$	0.05	12	9.880	9.820	-
	0.10	6	38.886	38.630	-
	0.15	4	87.225	86.640	-
$[0^0/90^0]_s$	0.05	12	7.366	7.300	7.340
	0.10	6	28.608	28.350	28.490
	0.15	4	64.003	63.410	63.660

Table 2: Lateral buckling moment M_{cr} (Nm) of cantilever composite channel-section beams

Lay-ups	This study	Kim et al. [19]		
		ESMM [†]	Analytical	ABAQUS
$[0^0]_{16}$	19.177	17.557	17.557	17.432
$[15^0/-15^0]_{4s}$	19.540	18.189	-	18.026
$[30^0/-30^0]_{4s}$	18.390	17.989	-	17.776
$[45^0/-45^0]_{4s}$	15.134	15.822	-	15.618
$[60^0/-60^0]_{4s}$	12.431	13.274	-	13.130
$[75^0/-75^0]_{4s}$	11.026	11.081	-	10.997
$[0^0/90^0]_{4s}$	15.363	14.333	14.333	14.220
$[0^0/-45^0/90^0/45^0]_{2s}$	15.228	15.237	-	15.043

[†] Exact stiffness matrix method

14

Table 3: Material and geometric properties of laminated channel-section beams

Parameter	Value
E_1	$15E_2$
E_2	1 GPa
G_{12}	$0.6E_2$
G_{23}	$0.3E_2$
ν_{12}	0.25
t_f	4 mm
t_w	4 mm
Ply thickness	0.25 mm
A^*	800 mm^2

Table 4: GA parameters for a typical run for optimisation of channel-section beams

Parameter	Value
Population size	120
Max. generation	100
γ_1	10^8
γ_2	10^8
γ_3	10^8
Crossover rate	0.5

Table 5: Vibration optimisation results for S-S beams with design variables of θ_1, θ_2, b, d

Case	Lay-ups	L (m)	Optimisation results							
			θ_1	θ_2	b (mm)	d (mm)	ω_1 (rad/s)	d/b	L/d	A/A^*
1	$[\theta_1/-\theta_1]_{4s}$	4.0	20^0	-	60	80	2176.0	1.3	50.0	1.0
		6.0	19^0	-	65	70	1067.9	1.1	85.7	1.0
		8.0	14^0	-	65	70	631.2	1.1	114.3	1.0
		10.0	10^0	-	65	70	415.1	1.1	142.9	1.0
		12.0	2^0	-	60	80	272.9	1.3	150.0	1.0
2	$[\theta_1/-\theta_2]_{4s}$	4.0	28^0	6^0	60	80	2199.1	1.3	50.0	1.0
		6.0	26^0	4^0	65	70	1080.7	1.1	85.7	1.0
		8.0	18^0	3^0	65	70	637.7	1.1	114.3	1.0
		10.0	13^0	4^0	65	70	416.7	1.1	142.9	1.0
		12.0	2^0	2^0	60	80	272.9	1.3	150.0	1.0
3	$[\theta_1/-\theta_1/\theta_2/-\theta_2]_{2s}$	4.0	26^0	6^0	60	80	2228.9	1.3	50.0	1.0
		6.0	24^0	5^0	65	70	1093.9	1.1	85.7	1.0
		8.0	17^0	0^0	65	70	642.0	1.1	114.3	1.0
		10.0	12^0	4^0	65	70	418.0	1.1	142.9	1.0
		12.0	2^0	2^0	60	80	272.9	1.3	150.0	1.0
4	$[0^0]_{16}^{\dagger}$	4.0			50	100	1718.2	2.0	40.0	1.0
		6.0			50	100	857.0	2.0	60.0	1.0
		8.0			50	100	498.8	2.0	80.0	1.0
		10.0			50	100	319.2	2.0	100.0	1.0
		12.0			50	100	221.7	2.0	120.0	1.0

† Assumed regular design

Table 6: Vibration optimisation results for C-C beams with design variables of θ_1, θ_2, b, d

Case	Lay-ups	L (m)	Optimisation results							
			θ_1	θ_2	b (mm)	d (mm)	ω_1 (rad/s)	d/b	L/d	A/A^*
1	$[\theta_1/-\theta_1]_{4s}$	4.0	21^0	-	50	100	3915.5	2.0	40.0	1.0
		6.0	20^0	-	55	90	1982.0	1.6	66.7	1.0
		8.0	21^0	-	60	80	1221.3	1.3	100.0	1.0
		10.0	17^0	-	60	80	818.4	1.3	125.0	1.0
		12.0	15^0	-	60	80	584.4	1.3	150.0	1.0
2	$[\theta_1/-\theta_2]_{4s}$	4.0	31^0	6^0	50	100	3961.6	2.0	40.0	1.0
		6.0	28^0	3^0	55	90	2006.6	1.6	66.7	1.0
		8.0	30^0	4^0	60	80	1233.7	1.3	100.0	1.0
		10.0	23^0	0^0	60	80	828.9	1.3	125.0	1.0
		12.0	18^0	0^0	60	80	591.5	1.3	150.0	1.0
										1.0
3	$[\theta_1/-\theta_1/\theta_2/-\theta_2]_{2s}$	4.0	29^0	3^0	50	100	4023.6	2.0	40.0	1.0
		6.0	27^0	0^0	55	90	2037.1	1.6	66.7	1.0
		8.0	28^0	0^0	60	80	1254.6	1.3	100.0	1.0
		10.0	21^0	2^0	60	80	838.0	1.3	125.0	1.0
		12.0	17^0	0^0	60	80	594.4	1.3	150.0	1.0
										1.0
4	$[0]_{16}^{\dagger}$	4.0			50	100	3568.3	2.0	40.0	1.0
		6.0			50	100	1645.6	2.0	60.0	1.0
		8.0			50	100	970.1	2.0	80.0	1.0
		10.0			50	100	655.1	2.0	100.0	1.0
		12.0			50	100	481.9	2.0	120.0	1.0

† Assumed regular design

Table 7: Vibration optimisation results for C-F beams with design variables of θ_1, θ_2, b, d

Case	Lay-ups	L (m)	Optimisation results							
			θ_1	θ_2	b (mm)	d (mm)	ω_1 (rad/s)	d/b	L/d	A/A^*
1	$[\theta_1/-\theta_1]_{4s}$	4.0	16^0	–	65	70	876.5	1.1	57.1	1.0
		6.0	10^0	-	65	70	411.3	1.1	85.7	1.0
		8.0	6^0	-	65	70	235.8	1.1	114.3	1.0
		10.0	2^0	-	65	70	152.3	1.1	142.9	1.0
		12.0	0^0	-	60	80	97.3	1.3	150.0	1.0
2	$[\theta_1/-\theta_2]_{4s}$	4.0	22^0	4^0	65	70	887.1	1.1	57.1	1.0
		6.0	13^0	0^0	65	70	413.0	1.1	85.7	1.0
		8.0	7^0	3^0	65	70	236.1	1.1	114.3	1.0
		10.0	2^0	2^0	65	70	152.3	1.1	142.9	1.0
		12.0	0^0	0^0	60	80	97.3	1.3	150.0	1.0
3	$[\theta_1/-\theta_1/\theta_2/-\theta_2]_{2s}$	4.0	21^0	0^0	65	70	896.1	1.1	57.1	1.0
		6.0	12^0	2^0	65	70	414.6	1.1	85.7	1.0
		8.0	7^0	0^0	65	70	236.6	1.1	114.3	1.0
		10.0	2^0	1^0	65	70	152.4	1.1	142.9	1.0
		12.0	0^0	0^0	60	80	97.3	1.3	150.0	1.0
4	$[0]_{16}^{\dagger}$	4.0			50	100	710.7	2.0	40.0	1.0
		6.0			50	100	315.9	2.0	60.0	1.0
		8.0			50	100	177.7	2.0	80.0	1.0
		10.0			50	100	113.7	2.0	100.0	1.0
		12.0			50	100	79.0	2.0	120.0	1.0

† Assumed regular design

Table 8: Lateral buckling optimisation results for S-S beams with design variables of θ_1, θ_2, b, d

Case	Lay-ups	L (m)	optimisation results							
			θ_1	θ_2	b (mm)	d (mm)	M_{cr} (Nm)	d/b	L/d	A/A^*
1	$[\theta_1/-\theta_1]_{4s}$	4.0	27^0	-	65	70	453.5	1.1	57.1	1.0
		6.0	29^0	-	65	70	290.1	1.1	85.7	1.0
		8.0	29^0	-	65	70	214.5	1.1	114.3	1.0
		10.0	29^0	-	65	70	170.4	1.1	142.9	1.0
		12.0	30^0	-	60	80	130.1	1.3	150.0	1.0
2	$[\theta_1/-\theta_2]_{4s}$	4.0	32^0	20^0	65	70	458.7	1.1	57.1	1.0
		6.0	33^0	22^0	65	70	292.9	1.1	85.7	1.0
		8.0	34^0	23^0	65	70	216.4	1.1	114.3	1.0
		10.0	34^0	23^0	65	70	172.0	1.1	142.9	1.0
		12.0	34^0	24^0	60	80	131.3	1.3	150.0	1.0
3	$[\theta_1/-\theta_1/\theta_2/-\theta_2]_{2s}$	4.0	36^0	0^0	65	70	476.3	1.1	57.1	1.0
		6.0	37^0	10^0	65	70	302.5	1.1	85.7	1.0
		8.0	37^0	13^0	65	70	223.1	1.1	114.3	1.0
		10.0	37^0	14^0	65	70	177.2	1.1	142.9	1.0
		12.0	37^0	14^0	60	80	135.2	1.3	150.0	1.0
4	$[0^0]_{16}^{\dagger}$	4.0			50	100	244.8	2.0	40.0	1.0
		6.0			50	100	122.9	2.0	60.0	1.0
		8.0			50	100	78.9	2.0	80.0	1.0
		10.0			50	100	57.5	2.0	100.0	1.0
		12.0			50	100	45.2	2.0	120.0	1.0

† Assumed regular design

Table 9: Lateral buckling optimisation results for C-C beams with design variables of θ_1, θ_2, b, d

Case	Lay-ups	L (m)	optimisation results							
			θ_1	θ_1	b (mm)	d (mm)	M_{cr} (N/m)	d/b	L/d	A/A^*
1	$\theta_1/-\theta_1]_{4s}$	4.0	14^0	-	65	70	1158.4	1.1	57.1	1.0
		6.0	25^0	-	65	70	642.1	1.1	85.7	1.0
		8.0	27^0	-	65	70	453.6	1.1	114.3	1.0
		10.0	28^0	-	65	70	353.3	1.1	142.9	1.0
		12.0	29^0	-	60	80	267.4	1.3	150.0	1.0
2	$\theta_1/-\theta_2]_{4s}$	4.0	23^0	0^0	65	70	1177.8	1.1	57.1	1.0
		6.0	31^0	14^0	65	70	651.2	1.1	85.7	1.0
		8.0	32^0	20^0	65	70	458.8	1.1	114.3	1.0
		10.0	33^0	21^0	65	70	356.9	1.1	142.9	1.0
		12.0	33^0	22^0	60	80	270.0	1.3	150.0	1.0
3	$[\theta_1/-\theta_1/\theta_2/-\theta_2]_{2s}$	4.0	26^0	0^0	65	70	1206.3	1.1	57.1	1.0
		6.0	34^0	0^0	65	70	678.4	1.1	85.7	1.0
		8.0	36^0	0^0	65	70	476.5	1.1	114.3	1.0
		10.0	37^0	7^0	65	70	369.3	1.1	142.9	1.0
		12.0	37^0	10^0	60	80	279.0	1.3	150.0	1.0
4	$[0^0]_{16}^{\dagger}$	4.0			50	100	895.0	2.0	40.0	1.0
		6.0			50	100	413.9	2.0	60.0	1.0
		8.0			50	100	244.9	2.0	80.0	1.0
		10.0			50	100	166.2	2.0	100.0	1.0
		12.0			50	100	122.9	2.0	120.0	1.0

$\dagger$ Assumed regular design

Table 10: Lateral buckling optimisation results for C-F beams with design variables of θ_1, θ_2, b, d

Case	Lay-ups	L (m)	optimisation results							
			θ_1	θ_2	b (mm)	d (mm)	M_{cr} (N/m)	d/b	L/d	A/A^*
1	$[\theta_1/-\theta_1]_{4s}$	4.0	27^0	-	65	70	244.0	1.1	57.1	1.0
		6.0	28^0	-	65	70	154.0	1.1	85.7	1.0
		8.0	29^0	-	65	70	112.5	1.1	114.3	1.0
		10.0	29^0	-	65	70	88.7	1.1	142.9	1.0
		12.0	29^0	-	60	80	67.4	1.3	150.0	1.0
2	$[\theta_1/-\theta_2]_{4s}$	4.0	32^0	19^0	65	70	246.7	1.1	57.1	1.0
		6.0	33^0	21^0	65	70	155.5	1.1	85.7	1.0
		8.0	33^0	22^0	65	70	113.5	1.1	114.3	1.0
		10.0	33^0	23^0	65	70	89.6	1.1	142.9	1.0
		12.0	33^0	23^0	60	80	68.0	1.3	150.0	1.0
3	$[\theta_1/-\theta_1/\theta_2/-\theta_2]_{2s}$	4.0	36^0	0^0	65	70	256.8	1.1	57.1	1.0
		6.0	37^0	0^0	65	70	161.1	1.1	85.7	1.0
		8.0	37^0	9^0	65	70	117.5	1.1	114.3	1.0
		10.0	37^0	11^0	65	70	92.5	1.1	142.9	1.0
		12.0	37^0	12^0	60	80	70.2	1.3	150.0	1.0
4	$[0^0]_{16}^{\dagger}$	4.0			50	100	108.4	2.0	40.0	1.0
		6.0			50	100	60.1	2.0	60.0	1.0
		8.0			50	100	40.7	2.0	80.0	1.0
		10.0			50	100	30.5	2.0	100.0	1.0
		12.0			50	100	24.3	2.0	120.0	1.0

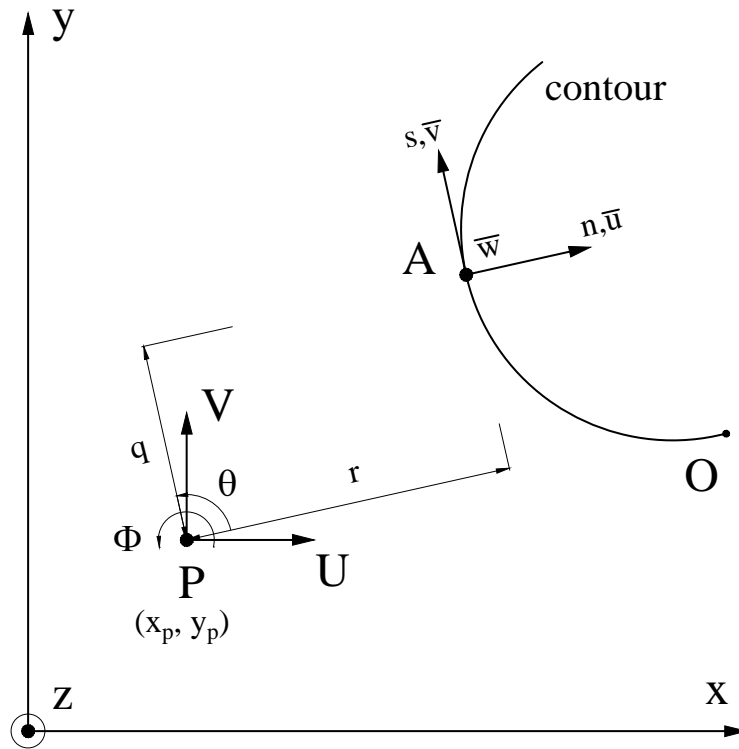† Assumed regular design

Figure Captions
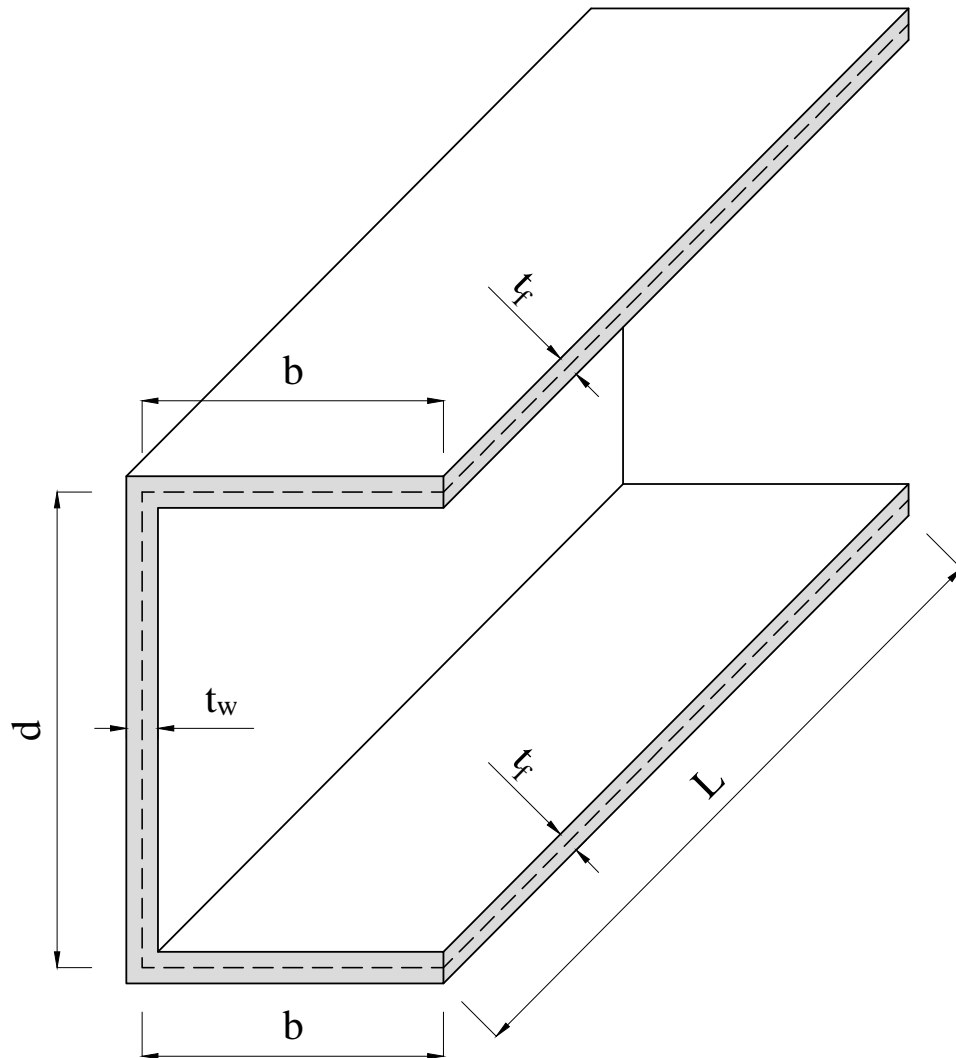
Figure 1. Coordinates for analysis of thin-walled beams.
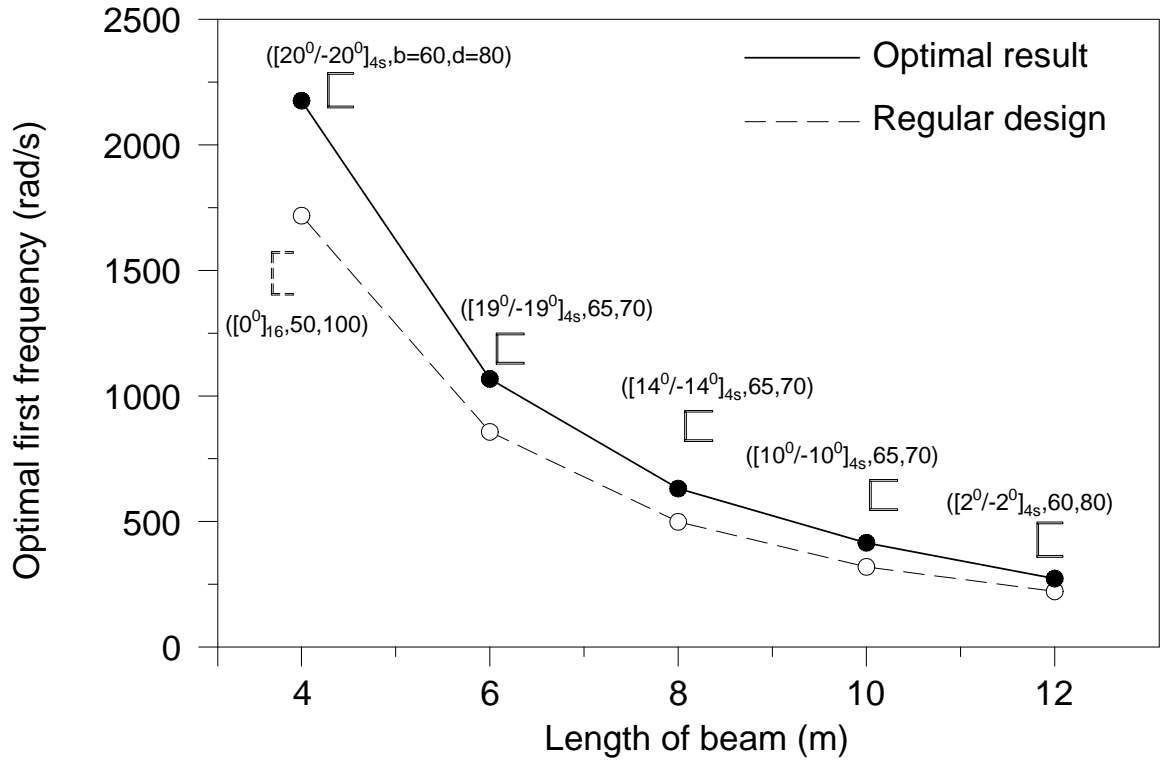
Figure 2. Geometry of a channel-section beam.

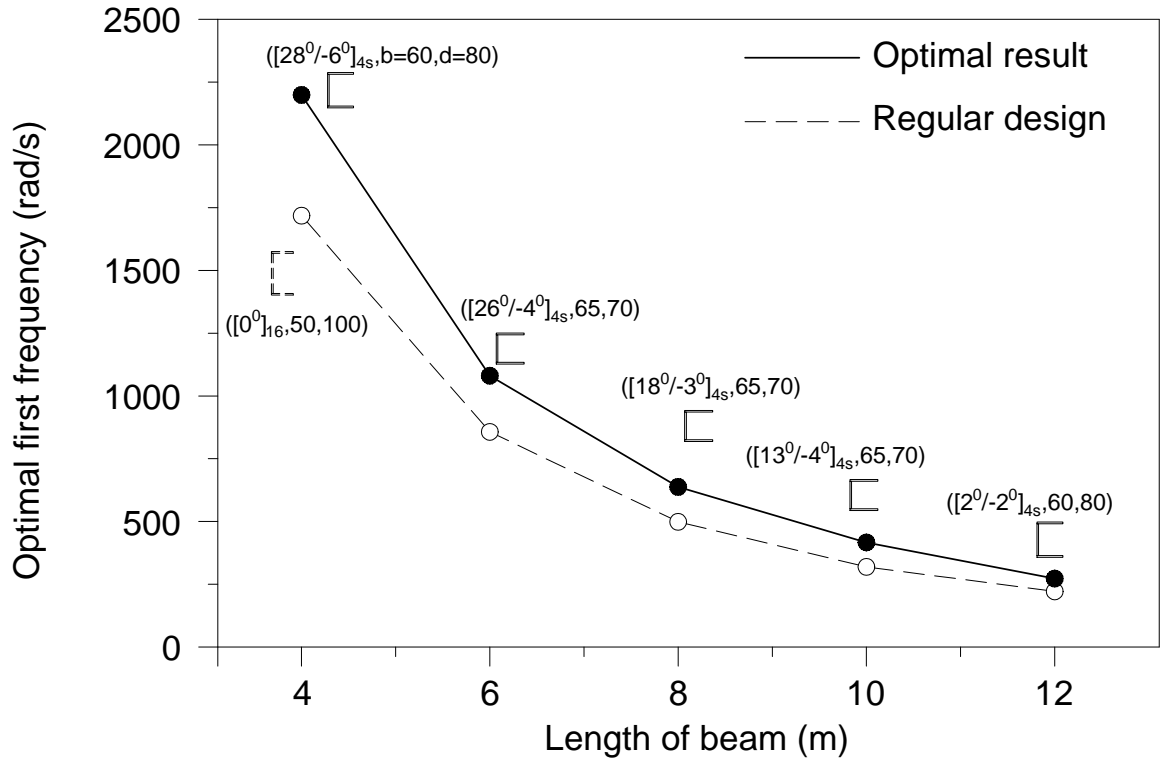Figure 3. Vibration optimisation results for S-S beams with $[\theta_1/-\theta_1]_{4s}$ lay-up.

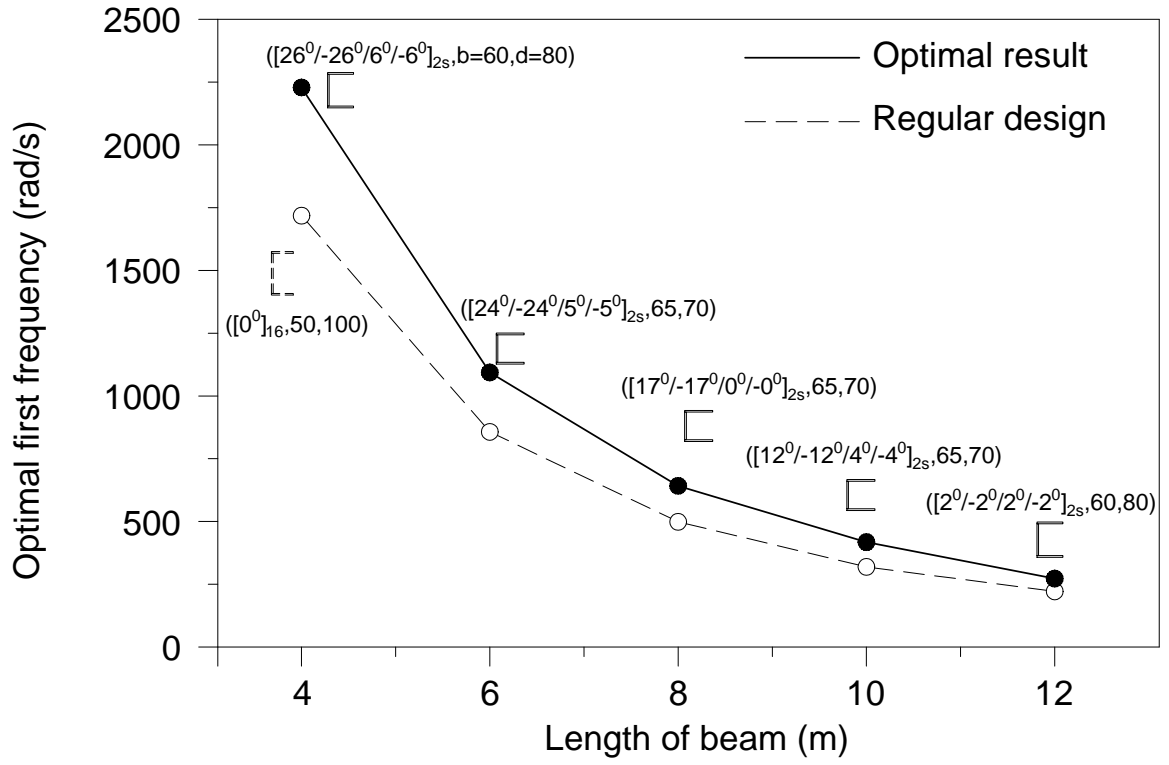Figure 4. Vibration optimisation results for S-S beams with $[\theta_1/-\theta_2]_{4s}$ lay-up.

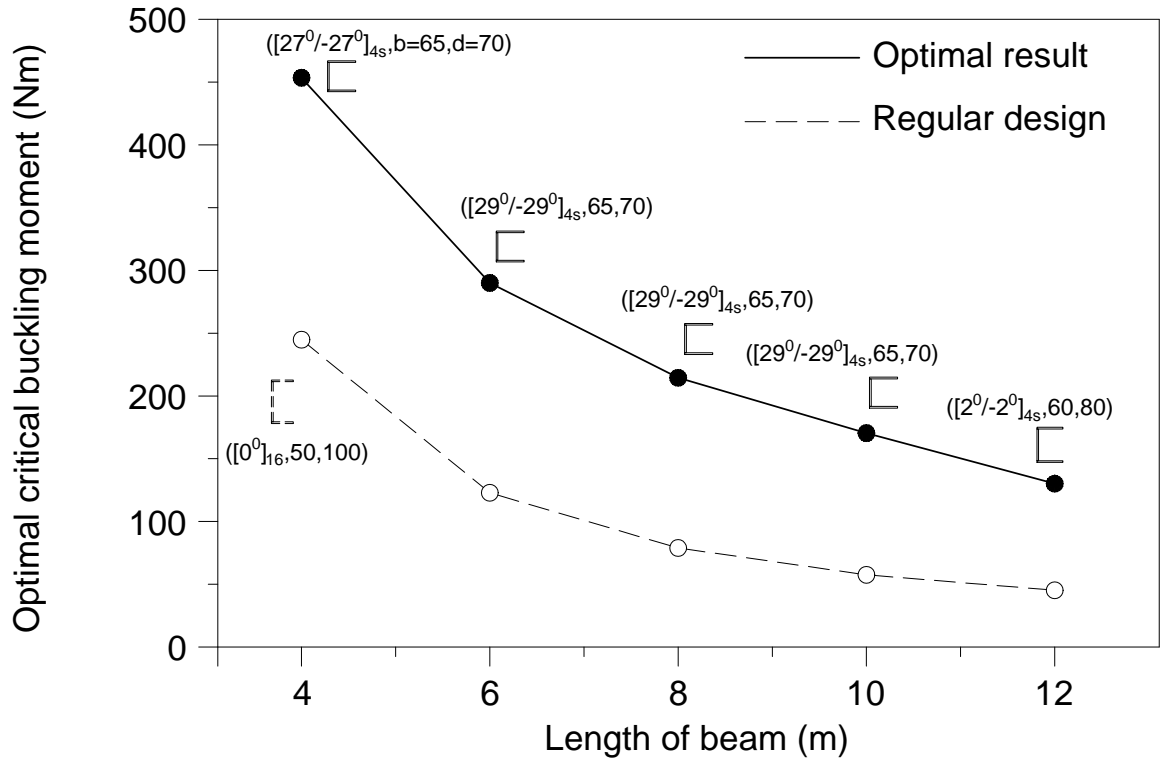Figure 5. Vibration optimisation results for S-S beams with $[\theta_1/-\theta_1/\theta_2/-\theta_2]_{2s}$ lay-up.

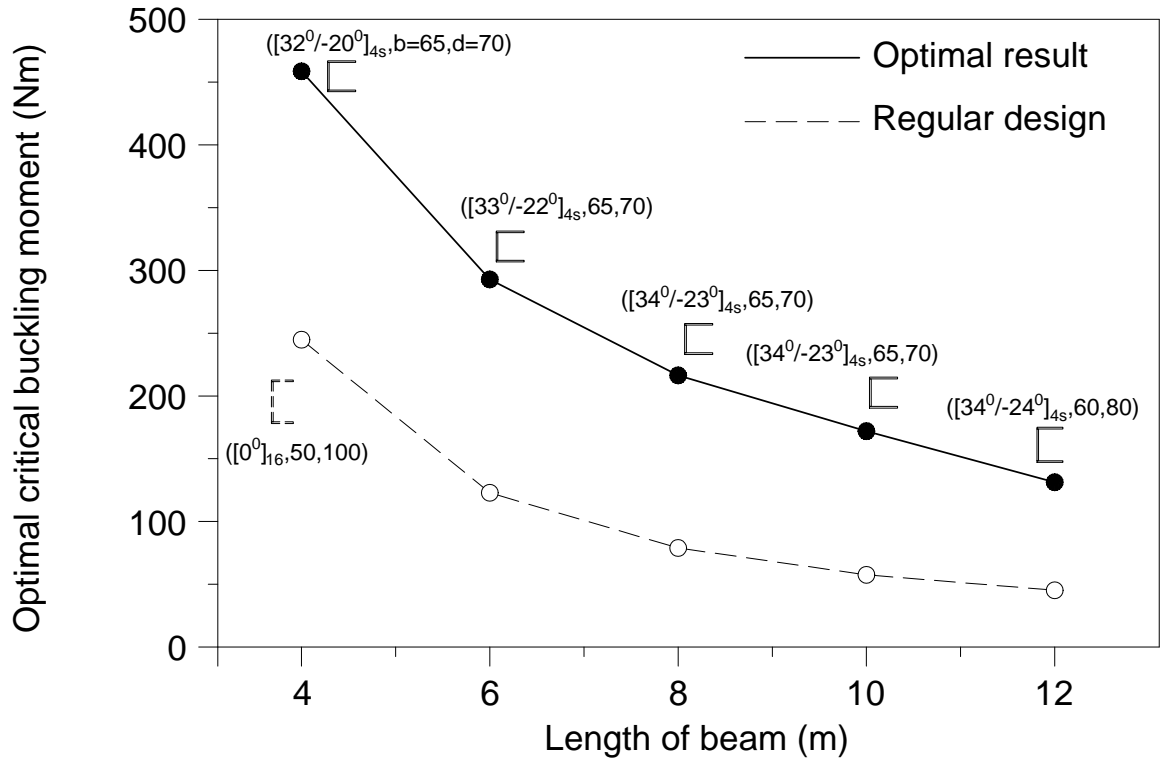Figure 6. Lateral buckling optimisation results for S-S beams with $[\theta_1/-\theta_1]_{4s}$ lay-up.

Figure 7. Lateral buckling optimisation results for S-S beams with $[\theta_1/-\theta_2]_{4s}$ lay-up.

Figure 8. Lateral buckling optimisation results for S-S beams with $[\theta_1/-\theta_1/\theta_2/-\theta_2]_{2s}$ lay-up.

Figure 9. Convergence history of Vibration optimisation of a 6m-long S-S beam with $[\theta_1/-\theta_1]_{4s}$ lay-up.

Figures

Figure 1: Coordinates for analysis of thin-walled beams.

Figure 2: Geometry of a channel-section beam.

Figure 3: Vibration optimisation results for S-S beams with $[\theta_1/-\theta_1]_{4s}$ lay-up.

Figure 4: Vibration optimisation results for S-S beams with $[\theta_1/-\theta_2]_{4s}$ lay-up.

Figure 5: Vibration optimisation results for S-S beams with $[\theta_1/-\theta_1/\theta_2/-\theta_2]_{2s}$ lay-up.

Figure 6: Lateral buckling optimisation results for S-S beams with $[\theta_1/-\theta_1]_{4s}$ lay-up.

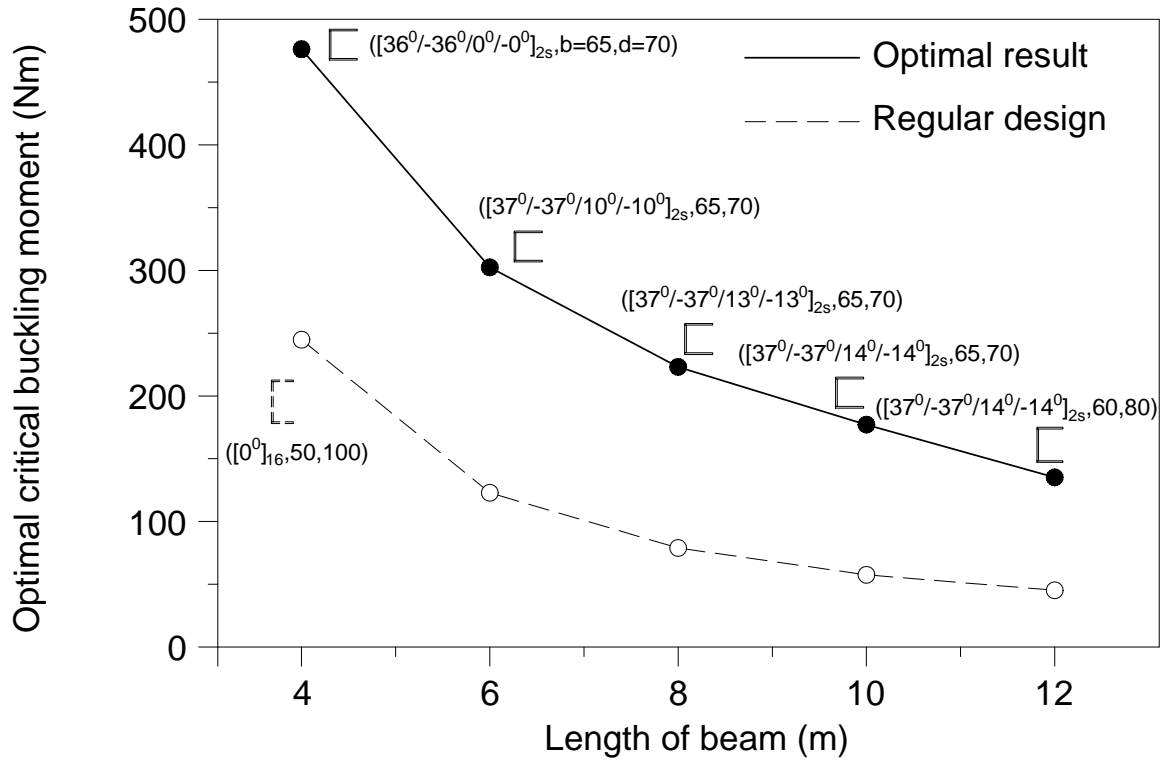Figure 7: Lateral buckling optimisation results for S-S beams with $[\theta_1/-\theta_2]_{4s}$ lay-up.

Figure 8: Lateral buckling optimisation results for S-S beams with $[\theta_1/-\theta_1/\theta_2/-\theta_2]_{2s}$ lay-up.
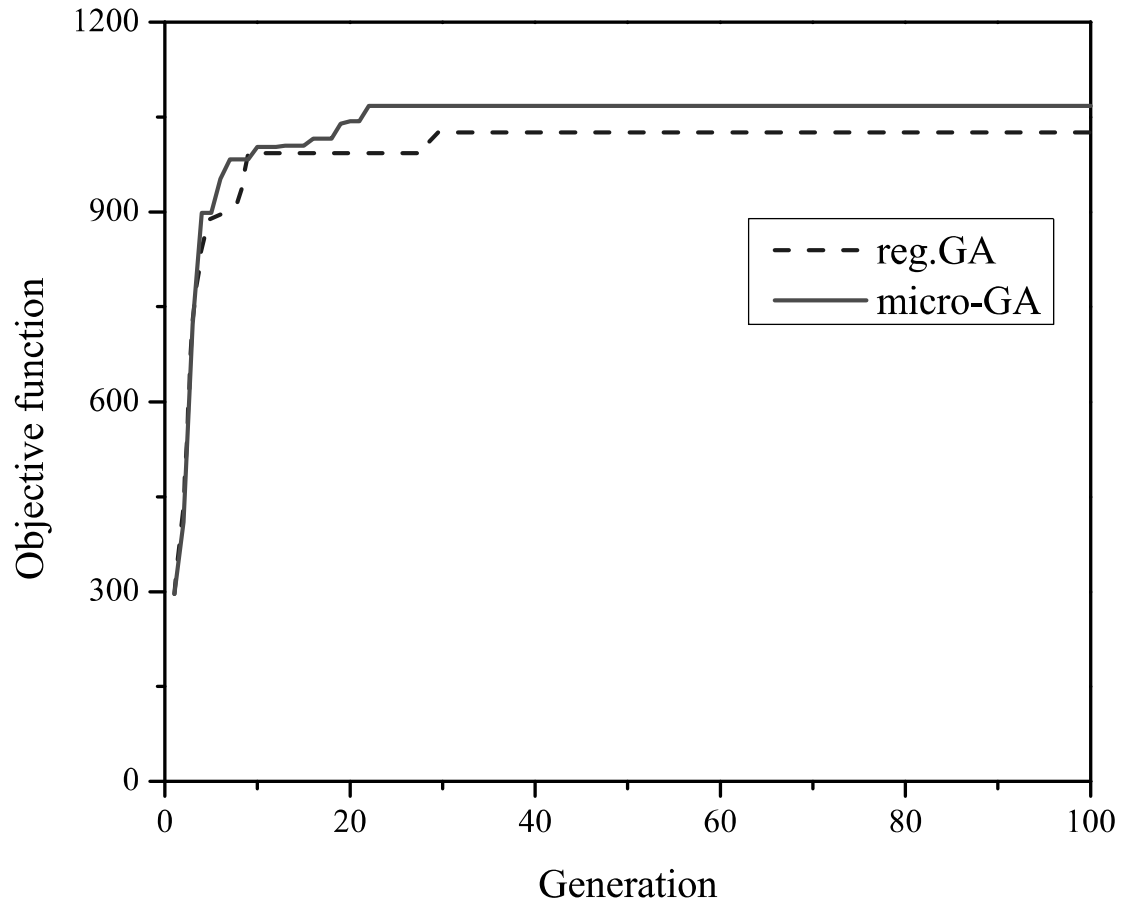
Figure 9: Convergence history of Vibration optimisation of a 6m-long S-S beam with $[\theta_1/-\theta_1]_{4s}$ lay-up.